Speciation of Basic Nitrogen Compounds in Gas Oils and Vacuum Gas Oils by Derivatization with BF 3 prior to NMR Analysis

Ludovic Chahen, Anne-Agathe Quoineaud, David Proriol, Séverine Artero, Mathieu Gilbert Vidalie, Frédéric Neyret-Martinez, Mickael Rivallan

▶ **To cite this version:**

Ludovic Chahen, Anne-Agathe Quoineaud, David Proriol, Séverine Artero, Mathieu Gilbert Vidalie, et al.. Speciation of Basic Nitrogen Compounds in Gas Oils and Vacuum Gas Oils by Derivatization with BF 3 prior to NMR Analysis. Energy & Fuels, 2017, 31 (10), pp.10752-10759. 10.1021/acs.energyfuels.7b01915 . hal-01702373

HAL Id: hal-01702373
https://ifp.hal.science/hal-01702373

Submitted on 9 Jun 2022

HAL is a multi-disciplinary open access archive for the deposit and dissemination of scientific research documents, whether they are published or not. The documents may come from teaching and research institutions in France or abroad, or from public or private research centers.

L'archive ouverte pluridisciplinaire **HAL**, est destinée au dépôt et à la diffusion de documents scientifiques de niveau recherche, publiés ou non, émanant des établissements d'enseignement et de recherche français ou étrangers, des laboratoires publics ou privés.

Distributed under a Creative Commons Attribution - NonCommercial 4.0 International License

Speciation of Basic Nitrogen Compounds in Gas Oils and Vacuum Gas Oils by Derivatization with BF_3 prior to NMR Analysis

L. Chahen,* A.-A. Quoineaud, D. Proriol, S. Artero, M. Vidalie, F. Neyret-Martinez, and M. Rivallan

IFP Energies nouvelles, Rond-point de l'échangeur de Solaize, BP 3, 69360 Solaize, France

ABSTRACT: Nitrogen-containing compounds, present in gas oils (GO) or vacuum gas oils (VGO) cuts, affect many of the important petroleum processes such as hydrocracking and hydrotreating due to their nucleophilic character. Basic nitrogen compounds, which can inhibit the acidic sites of the catalysts, are mainly pyridine derivatives (6-membered-ring nitrogen compounds), and despite the use of highly resolutive methods, their characterization, especially in VGO, is still limited. Herein, we propose a new promising methodology, coupling the derivatization with BF_3 of nonprotogenic nitrogen species and the use of NMR analysis. By crossing information from ^{19}F, ^{1}H, $^{1}H-^{19}F$ HMBC and ^{19}F DOSY, it is possible to determine the close environment of the nitrogen atom of the most nucleophilic nitrogen impurities in GO or in VGO cuts, independently of the sizes of the molecules. This approach allows the characterization and comparison of fingerprints of basic nitrogen impurities in charges or effluents.

Nitrogen-containing compounds, present in middle distillates cuts, affect many of the important petroleum processes such as hydrocracking and hydrotreating due to their nucleophilic character. These compounds may poison the catalysts used in hydrocracking, catalytic cracking, and reforming, through interactions with acid sites of catalysts and have a significant negative kinetic effect on hydrotreating reactions such as hydrodesulfurization (HDS). Thus, hydrodenitrogenation catalysts and processes (HDN) are well studied, and detailed knowledge of the type and concentration of N-compounds present in hydrocarbons cuts is required to optimize these HDN processes.

In middle distillates, most of the nitrogen is present as heterocycles with multiple aromatic rings. The N-compounds have been classified into two different groups: neutral and basic. Basic compounds, which can inhibit the acidic sites of the catalyst, are mainly pyridine derivatives (6-membered-ring nitrogen compounds) such as quinolines and acridines. Neutral compounds, among the most refractory species in HDN, are mainly pyrrole derivatives (5-membered-ring compounds) such as indoles and carbazoles.

Gas chromatography (GC) is definitely the most exploited technique to characterized nitrogen compounds in the petroleum cuts. GC can be coupled with a mass spectrometry detector, to take advantage of their high sensitivity, but nitrogen specific detectors, nitrogen chemiluminescence (NCD), and nitrogen phosphorus detectors (NPD) are definitely the most widely used.

For the diesel cut characterization, recent studies have demonstrated that GC×GC accomplishes better separations than GC, reducing the peak overlapping of N-compounds and therefore achieving better identifications and quantifications. However, despite the great resolution of GC×GC and the NCD detector, fractionation of the nitrogen species between neutral and basic nitrogen is preferable.[1,2] On heavier cuts like vacuum gas oil (VGO), even after fractionation of the basic-neutral nitrogen species, GC×GC-NCD shows difficulty to avoid overlapping of N-compounds.[3] Thus, the characterization of nitrogen compounds in hydrocarbons cuts is still limited and any complementary methods to improve their characterization are welcome.

In the case of basic nitrogen, since the most part of the compounds seems to be pyridine derivatives, a more specific method for characterizing this chemical function may be more useful. As a new approach, we propose to use Nuclear Magnetic Resonance (NMR) coupled with a chemical derivatization with BF_3 to characterize the nitrogen nonprotogenic functions present in middle distillates.

NMR is a powerful method to determine the chemical functions or the close environment of specific atoms. However, the NMR of the nitrogen ^{14}N or ^{15}N, though, is not trivial. ^{14}N is a medium sensitivity nucleus, but its signals are usually significantly broadened by quadrupolar interactions. ^{15}N yields sharp lines, but the 0.37% natural abundance of ^{15}N and its low gyromagnetic ratio ($\gamma = -27.126 \times 10^6$ T^{-1} s^{-1}) result in a major sensitivity penalty. Thus, it may be interesting to derivatize the nitrogen atom to analyze nitrogen functions by NMR.

Nitrogen atoms in organic compounds possess a free pair of electrons, and the nitrogen-containing organic molecules are considered as Lewis bases. They can react with the Lewis acid BF_3 to form Lewis adducts. The main advantage of BF_3 is that the isotopes ^{11}B and the ^{19}F have natural abundances of 80.1% and 100%, respectively. ^{11}B is a quadrupolar nucleus (spin 3/2) and gives generally broad bands which restrict strongly the analysis of mixture compounds. On the contrary, ^{19}F NMR (spin 1/2), as well as ^{1}H NMR, gives sharp bands and is very sensitive. Moreover, considering a Lewis adduct between one

nitrogen and one molecule of BF_3, the ^{19}F NMR will register a signal of 3 fluorine atoms for each nitrogen atom. Thus, the limits of detection will be lowered for ^{19}F NMR.

In the literature, the derivatization by BF_3, characterized by ^{19}F NMR, has already been used to indirectly measure the Lewis basicity of organic compounds or to identify structures of nitrogen[4−13] and oxygenated[14−19] adducts. However, to our knowledge, BF_3 has never been used as derivatization agent to characterize nitrogen compounds in feedstocks.

EXPERIMENTAL SECTION

Chemicals and Materials. All nitrogen compounds and $BF_3{\cdot}SMe_2$ were purchased from Sigma-Aldrich. CD_2Cl_2 was purchased from Euriso-top and dried on activated molecular sieves (3 Å). All manipulations were carried out under an inert atmosphere using Schlenk's technics. All other chemical compounds were used without further purifications. The silica used for the extraction was Merck silica (40−63 μm, 0.8 cm^3/g pore volume, 480−540 m^2/g). Silica is kept at 110 °C for at least 24 h before use. The real gas oil sample was obtained from a coker unit, and it contains 1200 mg of nitrogen/kg. The real vacuum gas oil was a straight run VGO, and it contained 1300 mg of nitrogen/kg.

^{19}F NMR and ^{19}F DOSY (Diffusion Ordered NMR Spectroscopy) spectra were obtained on a Bruker Avance 600 MHz spectrometer with a Quattro Nucleus Probe (QNP) of 5 mm at 298 K. 2D ^{19}F DOSY experiments were obtained using a bipolar gradient spin echo sequence (so-called PGSTE-BP).[20] The total diffusion encoding pulse duration δ was 2.5 ms, the delay for gradient recovery 1.0 ms, and the diffusion delay Δ 40 ms. Gradient amplitudes were used ranging from 0.7 to 29.3 $G{\cdot}cm^{-1}$, and 192 scans were recorded for each gradient amplitude. Heteronuclear Multiple-Bond Correlation spectroscopy (HMBC) experiments were carried out on a Bruker Avance 300 MHz spectrometer with a BroadBand probe for Fluoride Observation (BBFO) of 5 mm with a HMBC sequence using inverse detected $^1H/^{19}F$ long-range correlation with gradient selection and no decoupling during acquisition. Hexafluorobenzene was used as external reference chemical shift considering that $\delta_{C_6F_6} = -162.3$ ppm.

Derivatization Protocol. At room temperature, 0.05 mmol of nitrogen compound in 0.5 mL of CD_2Cl_2 was introduced into a Screw-Cap NMR sample tube of 5 mm in diameter. Next, 0.1 mmol of $BF_3{\cdot}SMe_2$ (2 equiv/nitrogen) in 0.1 mL of CD_2Cl_2 was added into the tube before being hermetically capped. The tube was slightly agitated manually for 2 min prior to NMR analysis.

Extraction Protocol on GO. The extraction protocol was inspired from the work of Lissitsyna et al.[2] An SPE propylene cartridge (diameter 1.6 cm) was manually packed with 5 g of Merck silica. The SPE cartridge was conditioned with 10 mL of hexane; then, 12 g of GO sample was applied to the silica SPE column. The cartridge was eluted successively with 90 mL of hexane, 110 mL of dichloromethane, and finally with 30 mL of acetone. The last fraction of acetone was dried on $MgSO_4$ and filtered, and acetone was evaporated to give an oily mixture containing 6.3 mg of nitrogen.

Derivatization of GO Fraction. The oily mixture from the SPE protocol was dissolved in 0.5 mL of CD_2Cl_2, and 0.111 mL of this solution was introduced into a Screw-Cap NMR sample tube of 5 mm in diameter. Next, 0.1 mmol of $BF_3{\cdot}SMe_2$ (1 equiv/nitrogen) in 0.1 mL of CD_2Cl_2 was added into the tube before being hermetically capped. The tube was agitated manually for 2 min prior to NMR analysis.

Analysis of GO Fraction by GC×GC-NCD. The acetone fraction of the GO has been analyzed by GC×GC-NCD according to the method published by Adam et al.[3] The acetone fraction of the GO contains quinolines (47% of total nitrogen), pyridines (25% of total nitrogen), acridines (16% of total nitrogen), indoles (4.6% of total nitrogen), anilines (4.2% of total nitrogen), and tetrahydroquinolines (3.35% of total nitrogen).

Extraction Protocol on VGO. An SPE propylene cartridge (diameter 1.6 cm) was manually packed with 5 g of Merck silica. The SPE cartridge was conditioned with 10 mL of hexane; then, 6 g of VGO, dissolved in 12 mL of hexane/toluene (50/50 in volume), was applied to the silica SPE column. The cartridge was eluted successively with 90 mL of hexane, 110 mL of dichloromethane, and finally with 30 mL of acetone. The protocol was done twice, and the fractions of acetone were gathered. Then, the final acetone fraction was dried on $MgSO_4$ and filtered, and acetone was evaporated to give an oily mixture containing 0.7 mg of nitrogen.

Derivatization of GO Fraction. The oily mixture from the SPE protocol was dissolved in 0.5 mL of CD_2Cl_2, and this solution was introduced into a Screw-Cap NMR sample tube of 5 mm in diameter. Next, 0.05 mmol of $BF_3{\cdot}SMe_2$ (1 equiv/nitrogen) in 0.1 mL of CD_2Cl_2 was added into the tube before being hermetically capped. The tube was agitated manually for 2 min prior to NMR analysis.

RESULTS AND DISCUSSION

Derivatization and NMR Methodologies. The purpose of this work is to validate qualitatively the concept of derivatization. The quantitative approach will be discussed in further studies.

In the VGO, the main impurities are sulfur and nitrogen compounds. BF_3 reacts with nonprotogenic and protogenic nitrogen compounds to form Lewis adducts with BF_3. However, in the presence of strong bases such as pyridine derivatives, protogenic adducts may undergo deprotonation of the nitrogen atom and form many different species.[21] Moreover, protogenic nitrogen species are generally weaker nucleophilic species and are not considered as responsible of catalysts deactivations. For these reasons, this work focuses on the study of nonprotogenic nitrogen species.

Maria et al.[22] have established a table of the enthalpies of adducts formation of nonprotogenic compounds with boron trifluoride in dichloromethane. The Lewis acid BF_3 forms quite stable adducts with basic nitrogen compounds ($-\Delta H°_{BF_3\text{-pyridine}}$ = 128.08 $kJ{\cdot}mol^{-1}$) in dichloromethane. According to Morris et al.,[23] dimethylsulfide has an enthalpy of formation of $-\Delta H°_{BF_3\text{-}SMe_2}$ = 14.6 $kJ{\cdot}mol^{-1}$ (pure gas-phase enthalpy). As a comparison, for tetrahydrothiophene (THT), the values of $-\Delta H°_{BF_3\text{-THT}}$ in the gas phase[23] and in dichloromethane solution[24] are, respectively, 22 and 52 $kJ{\cdot}mol^{-1}$. Thus, even if the enthalpy of formation of the adduct $BF_3{\cdot}SMe_2$ reaches $-\Delta H°_{BF_3\text{-}SMe_2}$ = 52 $kJ{\cdot}mol^{-1}$ in dichloromethane, nitrogen adducts are much more stable than $BF_3{\cdot}SMe_2$ or sulfur adducts.

$BF_3{\cdot}SMe_2$ is commercially available and is quite easy to handle as a solution. Thus, it has been used as derivative agent in the whole study.

Finally, dichloromethane interacts very slightly with BF_3 ($-\Delta H°_{BF_3\text{-}CH_2Cl_2}$ = 10.0 $kJ{\cdot}mol^{-1}$). This solvent is particularly well adapted to dissolve oil cuts, and most of the adducts of BF_3 with different pyridine derivatives seem to be soluble in dichloromethane. Therefore, dichloromethane-*d*2 has been used as solvent in the whole study.

Figure 1 shows the ^{19}F NMR spectrum of the BF_3-pyridine adduct at 25 °C.

The quartet observed is due to the spin−spin coupling with three fluorine nuclei and a ^{11}B boron nucleus ($^1J(^{11}B^{19}F)$ = 10.5 Hz). In addition, we may observe the presence of a broad and overlapped contribution due to the septet signal of the adduct formed between pyridine and the 19.9% of BF_3 owning the ^{10}B boron isotope (^{10}B spin = 3). Indeed, the ^{19}F NMR is able to detect both $^{11}BF_3$-pyridine and $^{10}BF_3$-pyridine. To avoid any confusion, the given ^{19}F NMR chemical shifts are always those related to $^{11}BF_3$ adducts.

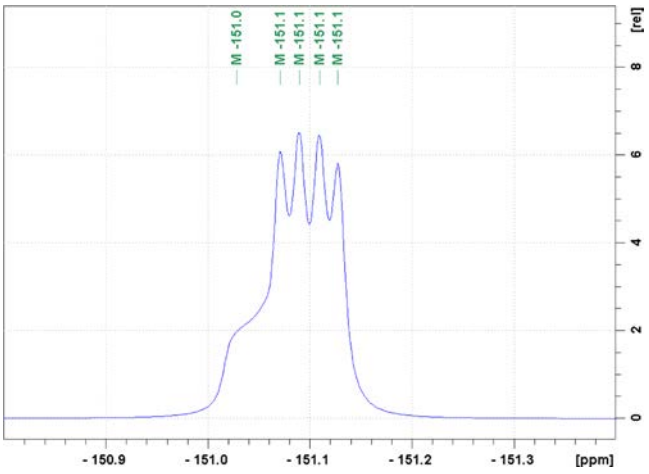

Figure 1. BF_3-pyridine adduct by ^{19}F NMR in CD_2Cl_2 at 25 °C.

In all model compounds spectra, there is always at least another significant signal. This peak is the residual signal of the excess of BF_3 forming adducts with remaining SMe_2, dichloromethane-*d*2, and eventual impurities due to products or manipulation like water. All of these adducts are in equilibrium, giving an average spectral contribution whose chemical shift can vary according to the nature of nitrogen species and from an experiment to another.

The BF_3 adducts of pyridine, 2,6-lutidine, quinoline, acridine, isoquinoline, 2,6-dimethylquinoline, *N*,*N*-dimethylaniline, phenanthridine, and triethylamine have been prepared and analyzed by ^{19}F NMR. The chemical shifts and *J*-coupling constants of the different BF_3 adducts are summarized in Table 1.

Table 1. Analysis of Different BF_3 Adducts by ^{19}F NMR at 25°C

adducts	average chemical shifts in ^{19}F NMR of 3 experiments (δ in ppm)	$^1J(^{11}B^{19}F)$ coupling constant in Hz
N,*N*-dimethylaniline	−157.7	13.1
pyridine	−151.1	10.5
isoquinoline	−150.8	10.4
quinoline	−144.8	12.3
phenanthridine	−144.6	12.1
2,6-dimethylquinoline	−133.9	15.1
2,6-lutidine	−136.3	14.2
acridine	−132.1	14.3

The spectral window is extended from −160 to −130 ppm. Many signals may overlap when the species are too similar, but contributions of great families like acridine, quinoline, or pyridine are sufficiently resolved to allow species distinction. *N*,*N*-Dimethylaniline has been selected to evaluate the impact of remaining aniline derivatives onto the analysis of pyridine derivatives. A dilution by 10 of the solution or an excess of 2 equiv of $BF_3{\cdot}SMe_2$ has no significant influence on the chemical shifts in ^{19}F NMR. However, due to the presence of $^{10}BF_3$ adducts, the signals are not well-defined and it is often easier to measure coupling constant on ^{11}B NMR than on ^{19}F NMR spectra.

The coupling constants depend on the adduct and thus may give also information on the corresponding chemical function. Considering only the pyridine derivatives, it seems that the coupling constant increases with the hindrance around the nitrogen atom. Indeed, in terms of hindrance around the nitrogen atom, we may consider the following order: 2,6-dimethylquinoline ∼ acridine ∼ 2,6-lutidine > quinoline ∼ phenanthridine > pyridine ∼ isoquinoline.

This hindrance effect seems to impact also chemical shifts since they follow the same order. Considering the work of Fratiello et al., the chemical shifts depend mainly on the strength of the interaction between the nitrogen and the boron atoms.[6] Actually, this interaction depends both on the Lewis basicity of the nitrogen atom and on the hindrance. In this study, the nucleophilic character is defined as the resultant of these 2 parameters and allows us to graduate the tendency of a nitrogen compound to form a more or less stable Lewis adduct with BF_3. Table 2 shows the chemical shifts of different adducts of substituted pyridines.

The comparison of the chemical shifts between this work and the literature is not trivial since the spectra have been registered with different (i) BF_3 precursors, (ii) adducts concentrations, (iii) calibration methods, and (iv) temperatures. However, despite the different analysis conditions, differences of only +0.1 ppm for BF_3-pyridine and only +1.0 ppm for BF_3-2,6-lutidine adducts are observed when compared to literature results. Thus, the results obtained in the present conditions at 25 °C are in agreement with Fratiello's results[6] and could be compared for discussion.

The 3-alkyl- and 4-alkyl-pyridine adducts (−151.3 ppm), regardless of the length of the alkyl chain, have almost the same ^{19}F chemical shifts as that of BF_3-pyridine (−151.1 ppm). It demonstrates that the influence of alkyl groups is very weak at these positions. However, the 2-alkyl-pyridine adducts have very different ^{19}F chemical shifts. The 2-methyl-pyridine adduct has a ^{19}F chemical shift of −147.6 ppm, and the 2-$CH_2CH_2CH_3$-pyridine adduct has a ^{19}F chemical shift of −145.9 ppm. The ^{19}F chemical shifts in pyridine adducts depend mainly on the substitution in 2- and 6-positions also known as *ortho*-positions. Finally, in Table 2, it is possible to separate all the pyridine derivatives in three families: not substituted in the *ortho*-position, substituted in one *ortho*-position, and substituted in both *ortho*-positions. The ^{19}F spectra can be separated in 3 parts as shown in Figure 2.

The three parts are delimited by the chemical shifts of the model compounds. These limits are not strict, and they can slightly evolve with the study of other derivatives. Concerning the compounds substituted in one or two *ortho*-positions, it is unlikely to have an overlapping in the ^{19}F NMR shifts considering the large gap between the two parts. The chemical shifts of the nonsubstituted and the monosubstituted compounds are relatively close. However, Fratiello et al. have studied a very large number of pyridine derivatives and the quinoline derivatives seem to have higher chemical shifts.[6] Thus, it is unlikely that these limits evolve and, in the worst case, the overlapping should be minor.

A mix of acridine, 2,6-lutidine, quinoline, isoquinoline, and *N*,*N*-dimethylaniline has been derivatized with $BF_3{\cdot}SMe_2$ in CD_2Cl_2 and analyzed by ^{19}F NMR. The chemical shifts of these species are similar to those reported in Table 2 except for acridine and *N*,*N*-dimethylaniline adducts which are only shifted from +0.1 ppm. Thus, we assume that mixture formation has no effect on the chemical shifts of the BF_3 adducts of the nonprotogenic nitrogen species.

The chemical shifts of the BF_3 adducts in ^{19}F NMR give information about the chemical form, about the hindrance of

Table 2. Chemical Shifts of Different BF_3 Adducts by ^{19}F NMR in CD_2Cl_2[a]

Nitrogen Compounds	Chemical Shifts of the BF_3 adducts in ppm	T (°C)	Ortho-substitution
Acridine	**-132.1**	**25**	Di-*ortho* substituted
2,6-dimethylquinoline	**-133.9**	**25**	Di-*ortho* substituted
2,6-lutidine	**-136.3**	**25**	Di-*ortho* substituted
2,6-lutidine	-137.3	**-10**	Di-*ortho* substituted
Phenanthridine	**-144.6**	**25**	Mono-*ortho*-substituted
Quinoline	**-144.8**	**25**	Mono-*ortho*-substituted
2-CH=CH_2-pyridine	-145.5	**-40**	Mono-*ortho*-substituted
2-$CH_2CH_2CH_3$-pyridine	-145.9	**-40**	Mono-*ortho*-substituted
2-CH_2CH_3-pyridine	-146.0	**-40**	Mono-*ortho*-substituted
2-CH_3-pyridine	-147.6	**-40**	Mono-*ortho*-substituted
2,4-$(CH_3)_2$-pyridine	-147.7	**0**	Mono-*ortho*-substituted
2,5-$(CH_3)_2$-pyridine	-147.8	**0**	Mono-*ortho*-substituted
2-CN-pyridine	-147.9	**0**	Mono-*ortho*-substituted
2-OCH_3-pyridine	-148.6	**0**	Mono-*ortho*-substituted
Isoquinoline	**-150.8**	**25**	No substitution in *ortho*
Pyridine	**-151.1**	**25**	No substitution in *ortho*
Pyridine	-151.2	**-40**	No substitution in *ortho*
3-CH_3-pyridine	-151.3	**-40**	No substitution in *ortho*
3-CH_2CH_3-pyridine	-151.3	**-40**	No substitution in *ortho*
4-CH_3-pyridine	-151.3	**-40**	No substitution in *ortho*
4-CH=CH_2-pyridine	-151.3	**0**	No substitution in *ortho*
4-CH_2CH_3-pyridine	-151.4	**-40**	No substitution in *ortho*
4-$C(CH_3)_3$-pyridine	-151.4	**0**	No substitution in *ortho*
3,5-$(CH_3)_2$-pyridine	-151.5	**-40**	No substitution in *ortho*
N,N-dimethylaniline	**-157.7**	**25**	-

[a]The results given in bold have been obtained in this study, and the other results have been obtained by Fratiello et al.[6]

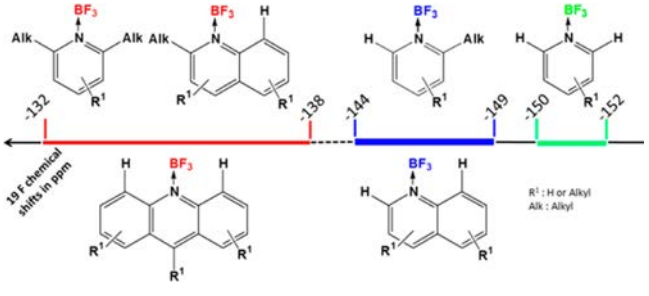

Figure 2. ^{19}F NMR chemical shifts ranges of pyridine derivatives adducts with BF_3.

the nitrogen compounds and, so, about their nucleophilic character. The common methods used to characterize the nitrogen compounds in GO cannot give such information. For example, GC×GC-NCD, which is certainly one of the most powerful techniques to reach molecular detail, is able to give the total amount of pyridines, quinolines, and acridines in a GO cut. However, GC×GC-NCD is unable to determine which part of these compounds are not too hindered to chelate a metal site and to poison an HDS catalyst for example.

Thus, this new approach 1D-NMR looks promising to compare the most nucleophilic nitrogen impurities in GO cuts and may be useful to find descriptors to anticipate the deactivation of certain catalysts. However, in most cases, the 1D-NMR does not give information about the size of the species which may be a crucial parameter considering the inhibition of catalytic sites in porous materials. Thus, to go further and to test the limits of this approach, real samples have been analyzed in ^{19}F DOSY. This 2D-NMR experiment allows us to separate compounds by their self-diffusion coefficients which depend generally strongly on the sizes of the molecules.

Preliminary Results on Very Polar Fractions of Real Hydrocarbons Cuts. A gas oil and a vacuum gas oil have been submitted to the Solid Phase Extraction (SPE) protocol described in the Experimental Section. The acetone fraction contains the most polar species and so, the most polar nitrogen compounds such as pyridines, quinolines, and acridines derivatives. For the GO, the acetone fraction has been analyzed by GC×GC-NCD according to the protocol proposed by Adam et al.[3] and contains mainly acridines (16% of total nitrogen), pyridines (25% of total nitrogen), and quinolines (47% of total nitrogen).

DOSY ^{19}F experiments have been carried out on the most polar fraction of gas oil and vacuum gas oil derivatized with $BF_3{\cdot}SMe_2$. To our knowledge, no ^{19}F DOSY experiments have been carried out on BF_3 adducts in the literature. Figures 3 and 4 show the ^{19}F DOSY spectra of the most polar fraction of the real gas oil and the real vacuum gas oil, both derivatized with $BF_3{\cdot}SMe_2$.

At the top of Figure 3, the ^{19}F NMR spectrum of the most polar derivatized nitrogen compounds shows signals from −155

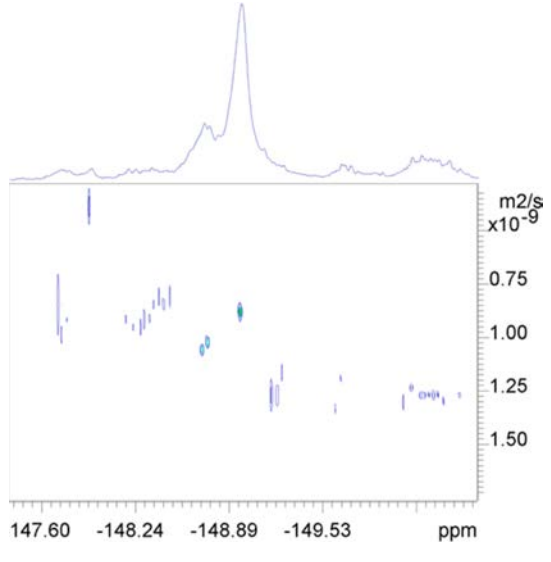

Figure 3. ^{19}F DOSY spectrum of the most polar fraction of the real gas oil derivatized with $BF_3{\cdot}SMe_2$ at 298 K.

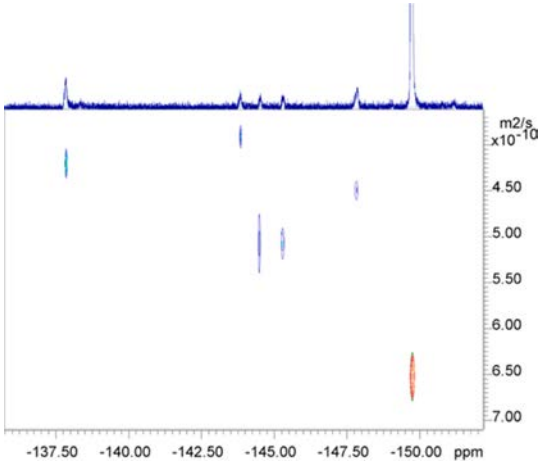

Figure 4. ^{19}F DOSY spectrum of the most polar fraction of the real vacuum gas oil derivatized with $BF_3{\cdot}SMe_2$ at 298 K.

to −147 ppm. The intense signal observed at −149.1 ppm in ^{19}F NMR indicates that a large amount of $BF_3{\cdot}SMe_2$ adduct remains in solution. Thus, in these conditions of preparation, all the nitrogen species have not been derivatized and, as expected, the ^{19}F NMR spectrum shows only the BF_3-adducts of the most nucleophilic nitrogen species. According to the chemical shift scale from Figure 2, the derivatized species are mainly non-*ortho*-substituted pyridines, mono-*ortho*-substituted pyridines, and non-*ortho*-substituted quinolines. This is in total agreement with the GC×GC-NCD results since quinolines and pyridines represent 72% of the total nitrogen in this GO. No signals are observed for adducts of *ortho*-substituted quinolines, di-*ortho*-substituted pyridines and acridines.

In Figure 3, the self-diffusion coefficients are held between $D = 3.78 \pm 1.08 \times 10^{-10}$ m^2/s and $D = 1.35 \pm 0.08 \times 10^{-9}$ m^2/s. Most of the species have self-diffusion coefficients relatively close, which is quite normal in a gas oil cut but the resolution is sufficient to notice tendencies. The self-diffusion coefficients are close to those observed by Kapur et al.[25] for the aromatic fraction of a diesel sample in $CDCl_3$ by ^1H DOSY. Thus, the presence of BF_3 seems to have a moderate impact on the self-diffusion coefficient and it is unlikely that the observed species are agglomerated adducts.

The signal at −149.0 ppm and at $D = 8.7 \pm 0.26 \times 10^{-10}$ m^2/s represents the remaining $BF_3{\cdot}SMe_2$. As expected, the highest self-diffusion coefficients are obtained for the species with smaller chemical shifts in ^{19}F NMR ($\delta < -149.0$ ppm), i.e., for the most stable small pyridine adducts with the shortest N−B bond. Consequently, it is logical that the weaker adducts, at higher chemical shifts ($\delta > -149.0$ ppm) and with longer N−B bonds, have weaker self-diffusion coefficients. However, surprisingly, $BF_3{\cdot}SMe_2$ which is certainly the smallest and the less stable adduct in the derivatized GO has an intermediate self-diffusion coefficient. Thus, in the case of BF_3 adducts, the size of the adduct does not seem to be the only parameter which governs the self-diffusion coefficient. In the case of $BF_3{\cdot}SMe_2$, one hypothesis may be that the self-diffusion coefficient depends also on the interaction of the adduct with the solvent. CD_2Cl_2 forms very weak adducts with BF_3, but it is present in a large excess. In the case of strong adducts with nitrogen compounds, the BF_3 is strongly bound to the nitrogen atom and the interaction with the solvent is negligible. In less stronger adducts like $BF_3{\cdot}SMe_2$, the B−S bond is weaker and the BF_3 may be more perturbed by the solvent. One other hypothesis may be that $BF_3{\cdot}SMe_2$ undergoes constantly BF_3 exchange with other nitrogen species and thus, the self-diffusion coefficient is strongly impacted. Consequently, cautions must be taken to exploit ^{19}F DOSY spectra in CD_2Cl_2. The size of the adducts may be compared but only between species which have similar stabilities, i.e., close chemical shifts and same derivatized atom.

The signal at −147.9 ppm has a very low diffusion coefficient ($D = 3.78 \pm 1.08 \times 10^{-10}$ m^2/s) compared to the other adducts with similar chemical shifts. In this case, it indicates clearly that these species are bigger than the others. Thus, this signal corresponds certainly to quinoline adducts.

For the real VGO, at the top of Figure 4, the ^{19}F NMR spectrum shows relatively well-defined signals from −152 to −136 ppm. As in Figure 3, all the nitrogen species have not been derivatized and there is an intense signal in ^{19}F NMR at 149.8 ppm which corresponds to the remaining $BF_3{\cdot}SMe_2$. According to the chemical shift scale from Figure 2, the most nucleophilic nitrogen species of vacuum gas oil seem to be mainly *ortho*-substituted pyridines, quinolines, *ortho*-substituted quinolines, and acridines derivatives. These results are perfectly in line with those expected for a most polar fraction of vacuum gas oil (heavier molecular weights than in GO).

For the VGO in Figure 4, the diffusion coefficients are comprised between $4.04 \pm 0.15 \times 10^{-10}$ and $6.53 \pm 0.36 \times 10^{-10}$ m^2/s. In these conditions, the remaining $BF_3{\cdot}SMe_2$ has a self-diffusion coefficient of $D = 6.43 \pm 0.04 \times 10^{-10}$ m^2/s. The values of self-diffusion coefficients cannot be compared directly with those of the GO. However, the $BF_3{\cdot}SMe_2$ can be considered as an internal reference to compare qualitatively the self-diffusion coefficients of species between the GO and the VGO. In Figure 4, all the species have smaller self-diffusion coefficients than the $BF_3{\cdot}SMe_2$ and, thus, smaller than those observed in Figure 3. As expected, considering the average size of molecules, the adducts of the VGO have lower self-diffusion coefficients than the adducts of the GO.

As a complementary experiment of the ^{19}F NMR, the ^{19}F DOSY may be very interesting to compare the sizes of the most nucleophilic nitrogen species in real derivatized samples. The ^{19}F DOSY experiment gives a more detailed "fingerprint" of the nitrogen species. This may facilitate the comparison of different samples and, potentially, the identification of key species in terms of nucleophilic character and also in terms of size of molecules. Moreover, with the help of a calibration based on model BF_3-adducts, it may be possible to evaluate the molecular weights of these species. However, CD_2Cl_2 is highly susceptible to convection and may disturb the evaluation of molecular weights during ^{19}F DOSY experiments.[26] The use of a hydrocarbon as solvent may simplify the correlation between the self-diffusion coefficient and the size of the nitrogen species.

In order to bring the most detailed "fingerprint" of basic nitrogen species, we have decided to go further with 2D-NMR experiments.

HMBC experiment correlates chemical shifts of two types of nuclei separated from each other with two or more chemical bonds. HMBC observes the scalar interactions through the chemical bonds. The most common HMBC experiment is $^1H-^{13}C$ HMBC which allows one to observe the ^1H in the first dimension and to correlate ^{13}C in the second dimension. Marchione et al.[27] have well studied $^1H-^{19}F$ 2D-NMR scalar coupling correlation pulse sequences on fluorinated organic compounds. More recently, Chenard et al.[28] have demonstrated

the Heteronuclear Overhauser Effect (HOESY) between the fluoride and the hydrogen atoms in BF_3-pyridine adducts. They have also realized $^1H-^{15}N$ and $^1H-^{13}C$ HMBC experiments on these adducts. However, to our knowledge, HMBC between fluoride and hydrogen atoms has never been used to study BF_3 adducts and to observe scalar correlations through the boron–nitrogen bond.

One of the main parameters in HMBC is the defocusing period which is optimized to be $1/2*^nJ(FH)$ and allows us to measuring long-range H–F coupling constants. It depends on the nuclei observed and the nature of the molecule. Indeed, this defocusing period is a compromised value which must be in the same order of the coupling constants observed. Consequently, as no information was available in the literature, it has been varied to find the optimum in each case.

HMBC experiments have been carried out to measure scalar correlations of the fluorine atoms of the BF_3 with the protons of the nitrogen compounds. Generally, it is recommended to observe the signal of the nucleus which has the larger spectral window, i.e., the fluorine atom, to obtain the best sensitivity and to lower the acquisition time of the experiment. The $^{19}F-^1H$ HMBC experiment (observation of the fluorine correlated to proton) of the BF_3-Pyridine adduct does not give any correlation. However, the $^1H-^{19}F$ HMBC experiment of the same adduct gives surprisingly a single $^5J_{FH}$ correlation between the fluorine atoms and the protons in the *meta*-position (positions 3 and 5) (see Figure 5). This correlation is well detected with defocusing periods of 2 and 4 Hz. The signal, observed with a defocusing period of 8 Hz, is less intense.

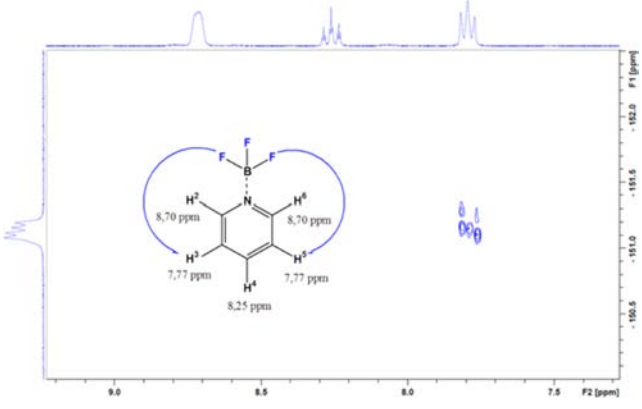

Figure 5. $^1H-^{19}F$ HMBC experiment (defocusing period of 4 Hz) of the BF_3-Pyridine adduct in CD_2Cl_2 at 298 K.

With defocusing delays of 4 and 8 Hz, the $^1H-^{19}F$ HMBC experiment of the BF_3-quinoline adduct shows 3 correlations (two $^4J_{FH}$ and one $^5J_{FH}$) between the fluorine atoms and the protons in positions 2, 8, and 3 (see Figure 6). By reducing this defocusing period to 2 Hz, it is possible to see another less intense $^6J_{FH}$ correlation between fluorine atoms and proton in position 7.

A mixture of BF_3-adducts of acridine, 2,6-lutidine, quinoline, isoquinoline, and *N,N*-dimethylaniline has been analyzed by $^1H-^{19}F$ HMBC to measure the eventual cross effect between BF_3-adducts (see Figure 7).

The $^1H-^{19}F$ HMBC experiment of the mixture, with a defocusing period of 4 Hz, shows that the presence of the other adducts has no impact on the correlations between fluorine atoms and protons in the BF_3-quinoline adduct. Concerning

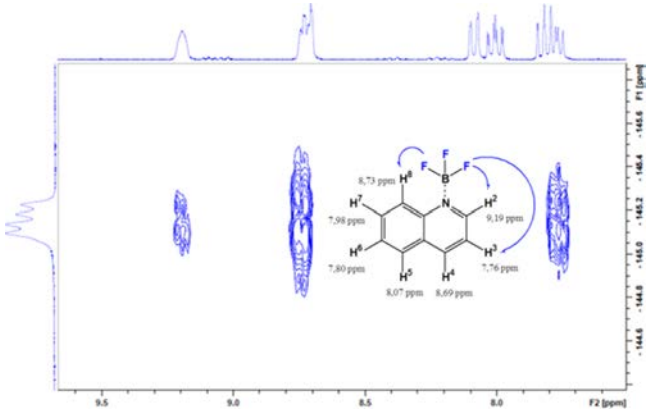

Figure 6. $^1H-^{19}F$ HMBC experiment (defocusing period of 4 Hz) of the BF_3-Quinoline adduct in CD_2Cl_2 at 298 K.

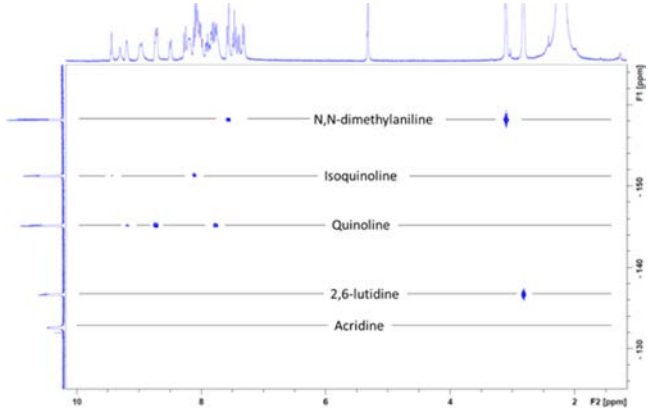

Figure 7. $^1H-^{19}F$ HMBC experiment (defocusing period of 4 Hz) of a mixture of BF_3-adducts in CD_2Cl_2 at 25 °C.

the BF_3-isoquinoline, as in BF_3-pyridine, the fluorine atoms correlate with the proton in the *meta*-position but also slightly with the protons in *ortho*-positions. In the BF_3-2,6-lutidine adduct, the protons in *meta*-positions (3 and 5 positions) do not correlate with the fluorine atoms. Thus, the presence of phenyl or alkyl groups on the pyridine ring greatly influences the correlations observed between the fluorine atoms and the aromatic protons.

The phenyl group increases the basicity of the nitrogen atom in the isoquinoline comparing to the pyridine. The N–B bond is maybe shorter in the isoquinoline adduct than in the pyridine adduct, and it explains certainly why it is easier to detect the correlation of the fluorine atoms with the protons in *ortho*-positions with a defocusing period of 4 Hz.

On the contrary, the hindrance of the two methyl groups around the nitrogen atom in 2,6-lutidine makes the coordination to the BF_3 certainly more difficult and the N–B bond must be longer than in the pyridine adduct. It explains certainly the lack of correlation between the fluorine atoms and the protons in *meta*-positions. The bond length explains also why no correlation is observed in the acridine adduct which has a higher chemical shift than BF_3-2,6-lutidine.

However, surprisingly, in the 2,6-lutidine adduct, there is a $^5J_{FH}$ correlation observed between the fluorine atoms and the aliphatic protons of the methyl groups. Thus, the $^1H-^{19}F$ HMBC experiments of BF_3 adducts allow also the detection of scalar correlation between fluorine atoms and aliphatic protons in *ortho*-positions.

Finally, the $^{1}H-^{19}F$ HMBC experiments of the BF_3-*N*,*N*-dimethylaniline adduct show that the fluorine atoms correlate also with aliphatic protons of the methyl groups but also with the protons in *meta*-positions even if aniline is not a heterocyclic compound.

To conclude, the $^{1}H-^{19}F$ HMBC experiments demonstrate that there are scalar correlations between the fluorine atoms of the BF_3 and the protons of the nitrogen compounds in BF_3 adducts. These correlations are measured through the N−B bond and allow the confirmation of the presence of protons on specific positions in pyridine or quinoline adducts. The correlations and, thus the information about the structure of the nitrogen compounds, depend mainly on the defocusing period used in the $^{1}H-^{19}F$ HMBC sequence. To analyze pyridine or quinoline adducts, it is recommended to vary the defocusing period between 2 and 8 Hz. However, with the $^{1}H-^{19}F$ HMBC sequences, no information is available on the BF_3-acridine adduct.

The $^{1}H-^{19}F$ HMBC experiments (using a defocusing period of 4 Hz) have been carried out on the basic nitrogen fraction of the real GO. The results are given in Figure 8. The ^{1}H spectra are presented on the abscissa, and the ^{19}F NMR spectra are presented on the ordinate.

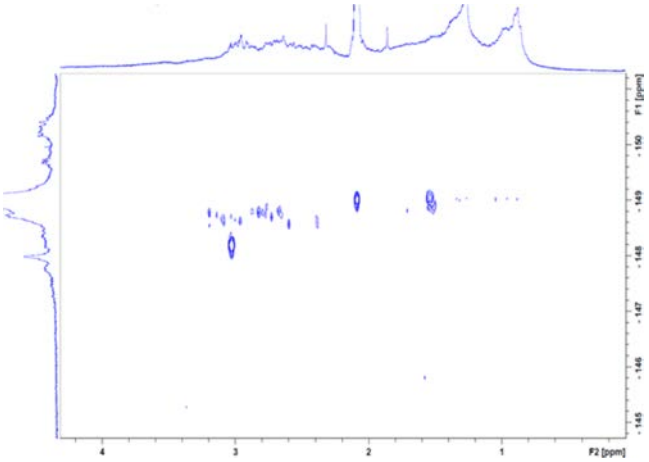

Figure 8. HMBC $^{1}H-^{19}F$ spectra (defocusing period of 4 Hz) of the most polar fraction of the real gas oil derivatized with $BF_3{\cdot}SMe_2$.

In Figure 8, the ^{1}H NMR shows significant broad signals of alkyl protons between 0.70 and 3.50 ppm and a very less intense broad signal for the aromatic protons.

For the derivatized fraction of GO, surprisingly, the scalar couplings observed in HMBC $^{1}H-^{19}F$ experiment are only concentrated between −149.5 and −148.0 ppm on the ordinate and 0.80 and 3.20 ppm on the abscissa. Therefore, these signals correspond only to the scalar couplings between the fluorine atoms with alkyl protons which represent largely the majority of protons in this GO fraction. Thus, this most polar fraction contains nitrogen species whose aromatic cycles are certainly very alkylated and the sample is certainly not concentrated enough to detect remaining aromatic protons. However, HMBC $^{1}H-^{19}F$ experiments give a lot of information about the nature of the alkyl groups.

The fluorine atoms couple mainly with protons whose ^{1}H chemical shifts are superior to 2.5 ppm. These chemical shifts are too high to be aromatic-CH_3 groups; thus, fluorine atoms couple with aromatic-CH_2 or aromatic-CH protons. Taking into account the ^{19}F NMR chemical shifts, this indicates that the main species are certainly mono-*ortho*-substituted pyridines alkylated at least with an ethyl group.

The couplings observed with protons, whose ^{1}H chemical shifts are comprised between 2 and 2.5 ppm, may be due to the couplings with the aromatic-CH_3 alkyl group. However, for the ^{1}H chemical shifts inferior to 2 ppm, the couplings might be due to longer scalar couplings than $^{5}J_{FH}$ with CH_3 groups.

Thus, the HMBC $^{1}H-^{19}F$ experiment can help to identify alkyl protons of nitrogen nucleophiles present in GO derivatized with $BF_3{\cdot}SMe_2$. With a more concentrated sample, the HMBC $^{1}H-^{19}F$ experiment may be also a very useful tool to identify the presence of certain aromatic protons. HMBC $^{1}H-^{19}F$ experiments have great potential to assist in the characterization of deactivating nitrogen species.

CONCLUSIONS

The methodology, coupling the derivatization with BF_3 of nonprotogenic nitrogen species and the use of NMR analysis, is very promising. By crossing information from ^{19}F NMR in 1D or 2D experiments, it is possible to determine the close environment of the nitrogen atom of the basic nitrogen species in gas oil or in vacuum gas oil cuts, independently of the sizes of the molecules. This approach allows one to establish "fingerprints" of the most nucleophilic nitrogen species which are likely to inhibit acidic sites. Then, by comparing highly and weakly deactivating samples, it would be possible to identify and to characterize specific species mainly responsible for the deactivation of the catalyst. Moreover, this approach is quite versatile. Indeed, the conditions of derivatization, $BF_3{\cdot}SMe_2$ as derivatization reagent and dichloromethane as solvent, allow the formation of BF_3-adducts with nitrogen species which have a certain level of nucleophilicity. By varying these conditions (derivatization reagent, solvent), it is possible to change the threshold in terms of nucleophilicity to observe more or less nucleophilic species.

AUTHOR INFORMATION

Corresponding Author

*E-mail: ludovic.chahen@ifpen.fr.

ORCID

L. Chahen: 0000-0002-0874-9871

Author Contributions

The manuscript was written through contributions of all authors. All authors have given approval to the final version of the manuscript.

Notes

The authors declare no competing financial interest.

REFERENCES

(1) Wiwel, P.; Hinnemann, B.; Hidalgo-Vivas, A.; Zeuthen, P.; Petersen, B. O.; Duss, J. Ø. *Ind. Eng. Chem. Res.* **2010**, *49*, 3184−3193.

(2) Lissitsyna, K.; Huertas, S.; Quintero, L. C.; Polo, L. M. *Fuel* **2013**, *104*, 752−757.

(3) Adam, F.; Bertoncini, F.; Dartiguelongue, C.; Marchand, K.; Thiebaut, D.; Hennion, M.-C. *Fuel* **2009**, *88*, 938−946.
(4) Mohajer, D.; Zakavi, S.; Rayati, S.; Zahedi, M.; Safari, N.; Khavasi, H. R.; Shahbazian, S. *New J. Chem.* **2004**, *28*, 1600−1607.
(5) Güizado-Rodríguez, M.; Ariza-Castolo, A.; Merino, G.; Vela, A.; Noth, H.; Bakhmutov, V. I.; Contreras, R. *J. Am. Chem. Soc.* **2001**, *123*, 9144−9152.
(6) Fratiello, A.; Vidulich, G. A.; Anderson, V. K.; Kazazian, M.; Stover, C. S.; Sabounjian, H. *J. Chem. Soc., Perkin Trans. 2* **1983**, 475−479.
(7) Fratiello, A.; Schuster, R. E. *Inorg. Chem.* **1968**, *7*, 1581−1585.
(8) Fratiello, A.; Schuster, R. E.; Geisel, M. *Inorg. Chem.* **1972**, *11*, 11−16.
(9) Heitsch, C. W. *Inorg. Chem.* **1965**, *4*, 1019−1024.
(10) Brinck, T.; Murray, J. S.; Politzer, P. *Inorg. Chem.* **1993**, *32*, 2622−2625.
(11) Cassoux, P.; Kuczkowski, R. L.; Serafini, A. *Inorg. Chem.* **1977**, *16*, 3005−3008.
(12) Hartman, J. S.; Miller, J. M. *Inorg. Chem.* **1974**, *13*, 1467−1471.
(13) Maria, P.-C.; Gal, J.-F.; de Franceschi, J.; Fargin, E. *J. Am. Chem. Soc.* **1987**, *109*, 483−492.
(14) Gillespie, R. J.; Hartman, J. S. *Can. J. Chem.* **1968**, *46*, 3799−3811.
(15) Gajewski, J. J.; Ngernmeesri, P. *Org. Lett.* **2000**, *2*, 2813−2815.
(16) Denmark, S. E.; Almstead, N. G. *J. Am. Chem. Soc.* **1993**, *115*, 3133−3139.
(17) Fratiello, A.; Vidulich, G. A.; Chow, Y. *J. Org. Chem.* **1973**, *38*, 2309−2314.
(18) Fratiello, A.; Schuster, R. E. *J. Org. Chem.* **1972**, *37*, 2237−2241.
(19) Fratiello, A.; Stover, C. S. *J. Org. Chem.* **1975**, *40*, 1244−1248.
(20) Pelta, M. D.; Barjat, H.; Morris, G. A.; Davis, A. L.; Hammond, S. *Magn. Reson. Chem.* **1998**, *36* (10), 706−714.
(21) Elter, G.; Neuhaus, M.; Meller, A.; Schmidt-Bäse, D. *J. Organomet. Chem.* **1990**, *381*, 299−313.
(22) Maria, P.-C.; Gal, J.-F. *J. Phys. Chem.* **1985**, *89*, 1296−1304.
(23) Morris, H. L.; Kulevsky, N. I.; Tamres, M.; Searles, S., Jr. *Inorg. Chem.* **1966**, *5*, 124−130.
(24) Gal, J.-F.; Maria, P.-C. *Prog. Phys. Org. Chem.* **1990**, *17*, 159−238.
(25) Kapur, G. S.; Findeisen, M.; Berger, S. *Fuel* **2000**, *79*, 1347−1351.
(26) Nilsson, M.; Morris, G. A. *J. Magn. Reson.* **2005**, *177*, 203−211.
(27) Marchione, A. A.; Dooley, R. J.; Conklin, B. *Magn. Reson. Chem.* **2014**, *52*, 183−189.
(28) Chenard, E.; Sutrisno, A.; Zhu, L.; Assary, R. S.; Kowalski, J. A.; Barton, J. L.; Bertke, J. A.; Gray, D. L.; Brushett, F. R.; Curtiss, L. A.; Moore, J. S. *J. Phys. Chem. C* **2016**, *120*, 8461−8471.